

Supporting information.

Fluorocarbons enhance intracellular delivery of short STAT3-sensors and enable specific imaging.

<u>Table of contents</u>	<u>pages</u>
1. HPLC purification of oligonucleotides and their properties	2 - 5
2. ODN duplex probes: melting properties	6 - 7
3. Fluorinated carriers for PF-ODN probes	8 - 9

1. HPLC purification

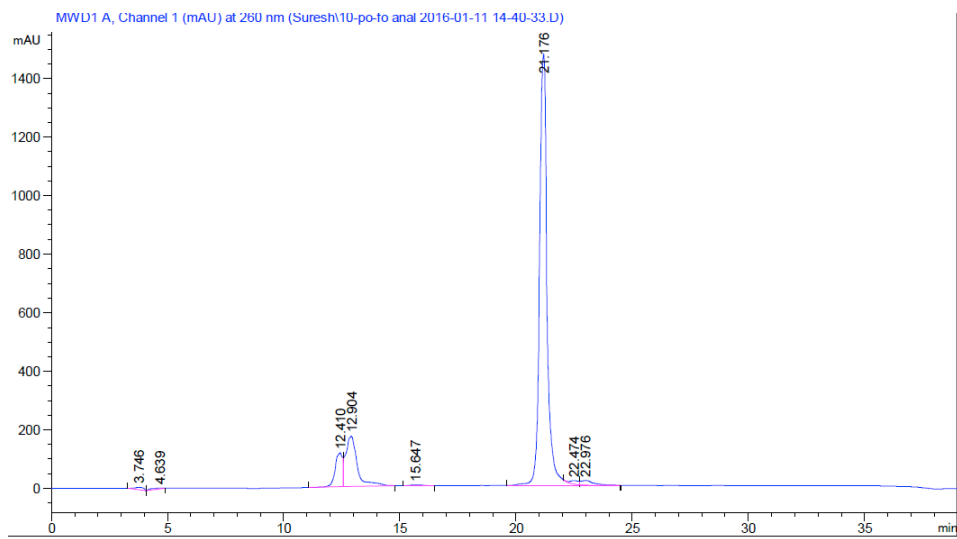


Figure S1A. HPLC analysis of the initial reaction mixture containing $\text{CF}_3(\text{CF}_2)_7\text{CH}_2\text{CH}_2\text{CH}_2\text{O-AGAGATTTAC*GGGAAATGGCT}$ (FO-ODN) product.

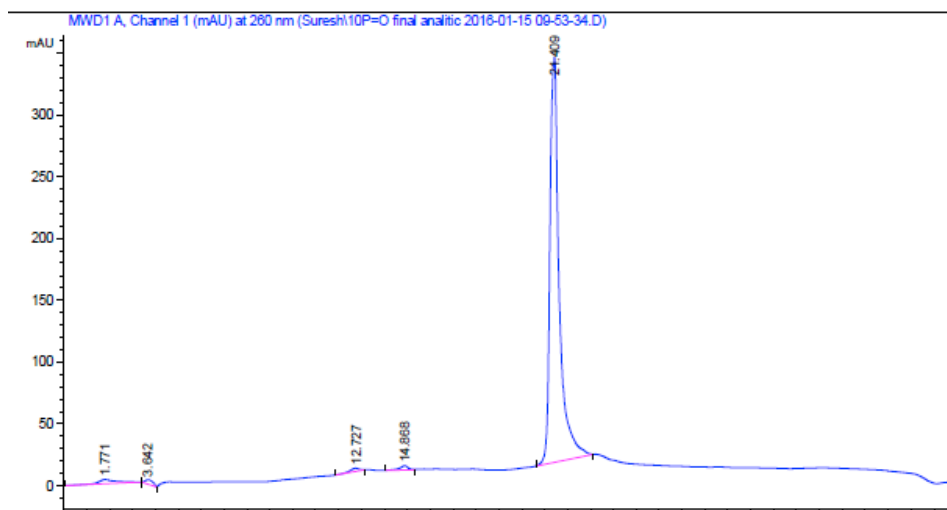


Figure S1B. HPLC analysis of purified $\text{CF}_3(\text{CF}_2)_7\text{CH}_2\text{CH}_2\text{CH}_2\text{O-AGAGATTTAC*GGGAAATGGCT}$ (FO-ODN).

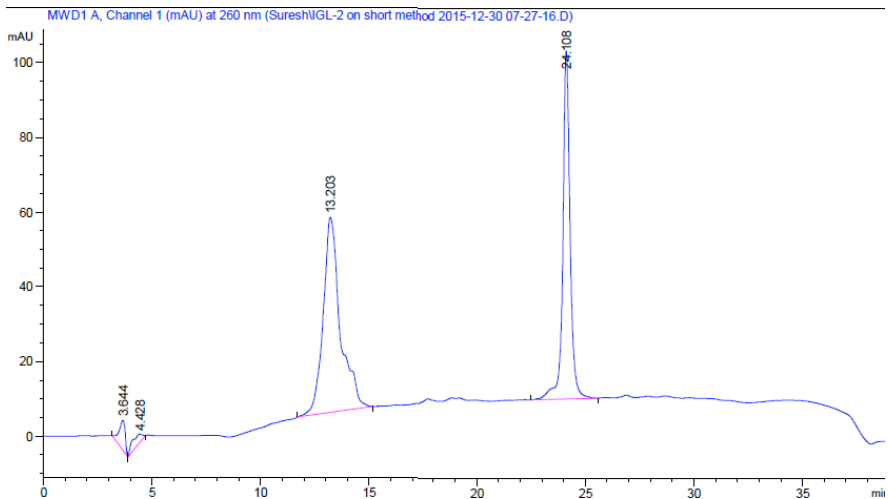


Figure S2. Analysis of oligonucleotide mixture after synthesis of $C_8F_{17}CH_2CH_2CH_2NHCO(CH_2)_9O$ -**CGAGATTTACGGGAAATGGCT** (FCN-ODN).

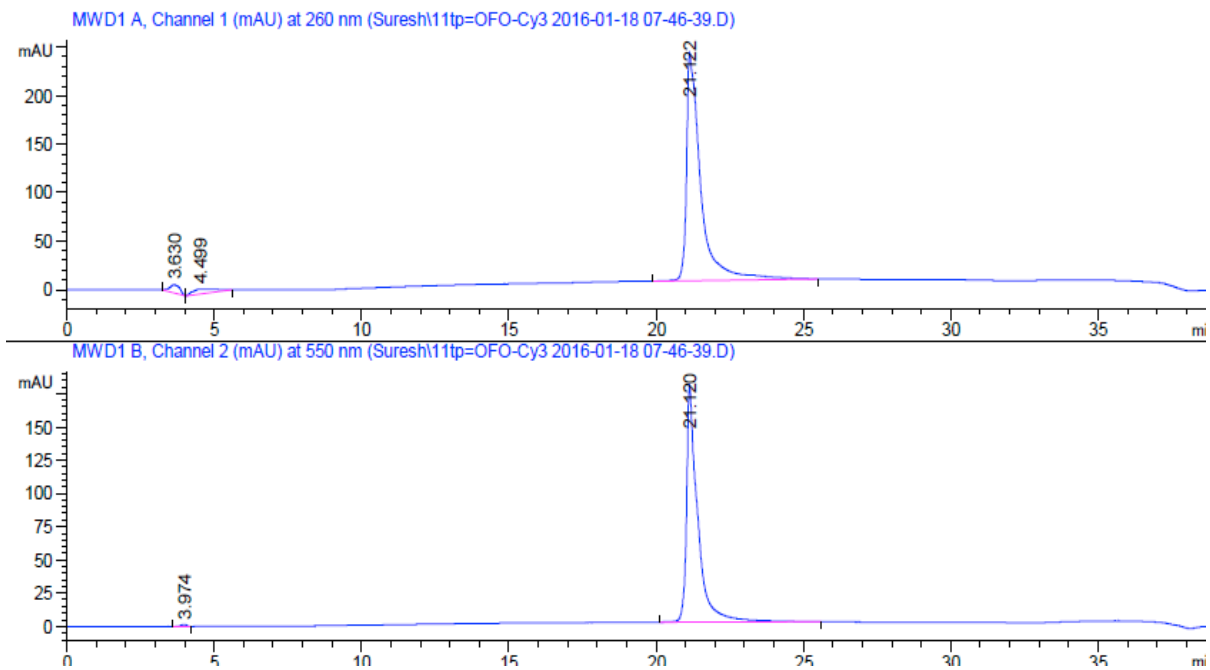


Figure S3. RP-HPLC analysis of FO-AGCC* Cy_3 ATTTCCCGTAAATCTCT on C18 column at 260 nm (up profile) and 550 nm (below).

Table S1. Retention times of pure modified ODNs on HPLC columns. Microsorb (MV 100-5CN) 250x4.6 mm or C18 HPLC columns were used for purification of FO- or FCN-oligonucleotides using identical protocols.

ODN	HPLC column, retention time (min)	
	C18	CN
Unprotected oligonucleotide	13.5	11.7-12.0
MeOTr- protected oligonucleotide	19.5	16.2
FO-oligonucleotide	21.4	17.5
FCN-oligonucleotide	24.0	19.3

2. ODN duplex melting properties.

Table S2. ODND probes used in this study and their melting points (T_m): fluorocarbon-free and FO or FCN -modified phosphodiester or hybrid phosphodiester/phosphorothioate ODN duplexes. Melting points were determined by Boltzmann sigmoidal least-squares non-linear fit ($r^2=0.95-0.98$) of experimental data.

N	Duplex	T_m in 0.01 M sodium phosphate, pH 7.4	+0.15 M NaCl
1	5' AGCC ATTTCCCGTAAATCTCT 3' 3' TCGGTAAAGGG CATT TAGAGAp(CH ₂) ₃ (CF ₂) ₇ CF ₃ 5'	53.2	65.2
2	5' AGCC*ATTTCCCGTAAATCTCT 3' 3' TCGGTAAAGGG CATT TAGAGAp(CH ₂) ₃ (CF ₂) ₇ CF ₃ 5' Cy3	50.8	63.0
3	5' AGCC ATTTCCCGTAAATCTCT 3' 3' TCGGTAAAGGG CATT TAGAGA 5'	52.8	63.8
4	5' CF ₃ (CF ₂) ₇ (CH ₂) ₃ p AGCC ATTTCCCGTAAATCTCT 3' 3' TCGGTAAAGGG CATT TAGAGAp(CH ₂) ₃ (CF ₂) ₇ CF ₃ 5' Cy3	55.9	-
5	Cy3 5' CF ₃ (CF ₂) ₇ (CH ₂) ₃ p AGCC ATTTCCCGTAAATCTCT 3' 3' TCGGTAAAGGG CATT TAGAGAp(CH ₂) ₃ (CF ₂) ₇ CF ₃ 5'	55.5	69.5
6	5' CF ₃ (CF ₂) ₇ (CH ₂) ₃ p AGCC ATTTCCCGTAAATCTCT 3' 3' TCGGTAAAGGG CATT TAGAGAp(CH ₂) ₃ (CF ₂) ₇ CF ₃ 5'	59.0	70.7
7	Cy3 5' AGCC ATTTCCCGTAAATCTCT 3' 3' TCGGTAAAGGG CATT TAGAGA 5'	-	62.0
8	Cy3 5' AGCC ATTTCCCGTAAATCTCT 3' 3' 3' TCGGTAAAGGG CATT TAGAGAp(CH ₂) ₃ (CF ₂) ₇ CF ₃ 5'	-	63.2
9	5' CF ₃ (CF ₂) ₇ (CH ₂) ₃ p AGCCAT TTCCCGTAAATCTCT 3' 3' TCGGTAAAGGG CATT TAGAGAp(CH ₂) ₃ (CF ₂) ₇ CF ₃ 5'	-	59.6

10	5' CF ₃ (CF ₂) ₇ (CH ₂) ₃ p AGCCAT TTCCC GTAAATCTCT 3' 3' TCGGTAAAGGG CATTTAGAGA p(CH ₂) ₃ (CF ₂) ₇ CF ₃ 5' Cy3		58.0
11	5' CF ₃ (CF ₂) ₇ (CH ₂) ₃ p AGCCAT TTCCCGTAAATCTCT 3' 3' TCGGTAAAGGG CATTTAGAGA 5'	-	58.9
12	5' CF ₃ (CF ₂) ₇ (CH ₂) ₃ p AGCCAT TTCCCGTAAATCTCT 3' 3' TCGGTAAAGGGCAT TTAGAGAp (CH ₂) ₃ (CF ₂) ₇ CF ₃ 5'	-	59.8
13	5' CF ₃ (CF ₂) ₇ (CH ₂) ₃ p AGCC ATTTCCCGTAAATCTCT 3' 3' TCGGTAAAGGG CATTTAGAGAp (CH ₂) ₃ (CF ₂) ₇ CF ₃ 5'	-	68.8
14	5' CF ₃ (CF ₂) ₇ (CH ₂) ₃ p AGCC ATTTCCCGTAAATCTCT 3' 3' TCGGTAAAGGG CATTTAGAGA 5'	-	67.8
15	5' CF ₃ (CF ₂) ₇ (CH ₂) ₃ p AGCCAT TTCCCGTAAATCTCT 5' 3' TCGGTAAAGGGCATT TAGAGC p(CH ₂) ₉ CONH(CH ₂) ₃ C ₈ F ₁₇ 3'	-	60.1
16	5' AGCC ATTTCCCGTAAATCTCT 5' 3' TCGGTAAAGGGCATT TAGAGC p(CH ₂) ₉ CONH(CH ₂) ₃ C ₈ F ₁₇ 3'	-	63.8

3. Perfluorinated carriers for PF-ODND probes.

Figure S4. An example of van der Waals (VDW) interaction between fluorinated groups linked to M5-gPLL-PFUDA and ODND. Modeling of interaction between 1FO-PS-Cy3 ODND and M5-gPLL-PFUDA fragment (n=50 mer) obtained using molecular dynamics simulations run in MOE as described in Materials and Methods. The simulations in MOE were performed by applying assisted model building with energy refinement (Amber10:EHT) force field in simulated water/NaCl solvent (layer, n=8). VDW surfaces (in atom colors) are shown as an overlay over the atoms of the FO moieties linked to ODND and M5-gPLL-PFUDA carrier.

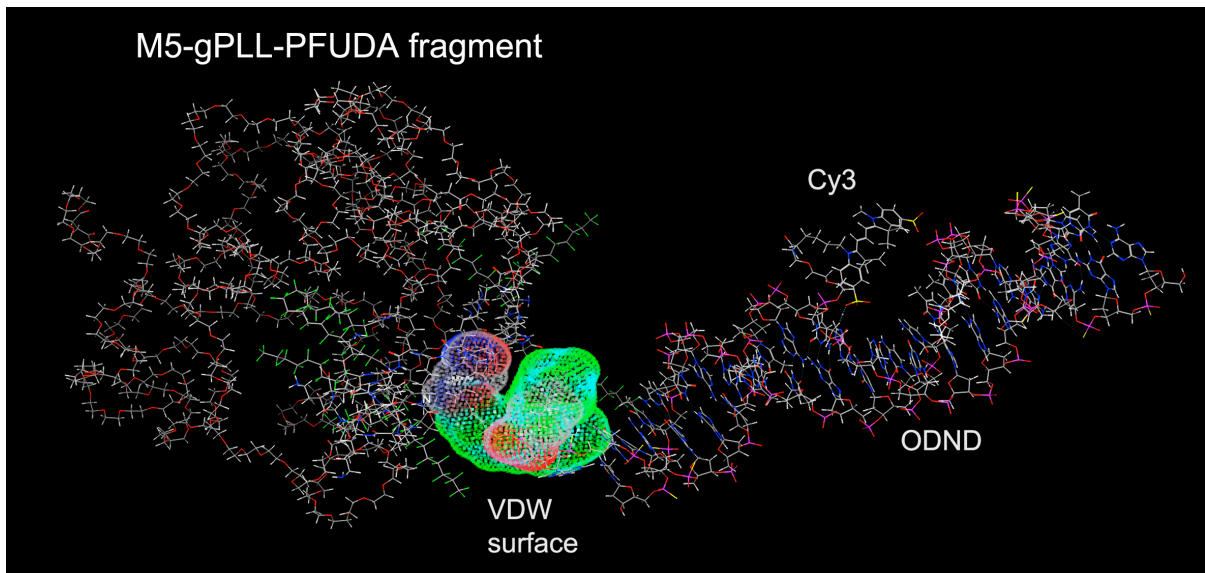


Figure S5. ^{19}F NMR spectroscopy and MRI of PFUDA standards and M5-gPLL-PFUDA. (A) ^{19}F NMR spectrum of PFUDA (20 mM) at 200 MHz; (B) ^{19}F NMR spectrum of the same sample as in A obtained using a 3T clinical scanner (Achieva, Philips); (C) ^{19}F NMR spectrum of M5-gPLL-PFUDA (6.6 mM PFUDA); (D) ^{19}F NMR spectrum of M5-gPLL-PFUDA (6.6 mM PFUDA) at 200 MHz (E) calibration curve showing the dependence of integrated ^{19}F spectroscopic peaks (integration window shown with grey vertical lines in B and C) from the concentration of PFUDA; (F) multi-slice imaging of M5-gPLL-PFUDA (6.6 mM PFUDA) using a 0.5 cm solenoid coil. The ^{19}F MR imaging parameters were: TR/TE = 300/0.12 ms; flip angle (FA) = 60° ; NSA = 32; 3 slices with slice thickness of 4 mm; field of view (FOV) of 30 mm \times 30 mm with matrix size of 60 \times 60 pixels.

